

Creep Rupture Strength of Rods Stretched in an Aggressive Medium with Various Two-Connected Forms of Their Cross-Sections

A. M. Lokoshchenko^{a,*}, L. V. Fomin^{a,c}, and N. S. Larin^{a,b}

^a*Research Institute of Mechanics, Moscow State University, Moscow, 119192 Russia*

^b*Federal State Budget Educational Institution of Higher Education, Moscow State University, Moscow, 119991 Russia*

^c*Samara State Technical University (Samara Polytech), Samara, Samara Oblast, 443100 Russia*

**e-mail: loko@imec.msu.ru*

Received November 11, 2019; revised July 30, 2020; accepted October 17, 2020

Abstract—The creep rupture strength of two-connected cross-section rods stretched in an aggressive medium is investigated. The cross-sections of the rods are considered, in which the shapes of the outer and inner contours are similar, in addition, the areas of the hollow (inner) part are 25% of the areas of the bordering outer, loaded part. The areas of the loaded parts of sections with different shapes coincide. To assess the influence of an aggressive medium on creep rupture strength, the Rabotnov kinetic theory is used. It works with two structural parameters (material damage and concentration of environmental elements in the rod material). To determine the level of an aggressive medium in the rods, approximate solutions of the diffusion equations are used, based on taking into account the motion of diffusion fronts from the outer and inner surfaces of the rods.

Keywords: stretched rods, kinetic theory, creep rupture strength, cross-section shape, time to fracture, damage, aggressive medium, diffusion equation, diffusion front

DOI: 10.3103/S0025654421070177

INTRODUCTION

Strict requirements for the quality and reliability of structures that are under high temperature loads for a long time lead to the need to predict the durability of their operation, taking into account various specific features that may arise in reality. One of the important factors that significantly affect the creep characteristics and creep rupture strength of metals is the working environment in which the structures under study or their individual elements are located. Test results generally show a significant degradation in metal performance due to exposure to such environments. Known studies of the influence of an aggressive environment on the creep and creep rupture strength of metals show that this influence is mainly characterized by diffusion and corrosion processes occurring in the metal [1].

A detailed analysis of the features of the mechanical behavior of metals under a long-term high-temperature loaded state in aggressive media and the main phenomenological approaches used in modeling the effect of the environment on creep and creep rupture strength is presented [2].

Rods with such simply connected cross-sections, for which the minimum dimensions coincided, were considered in [3]. In this case, the influence of the shape of the cross-section of the rod on the concentration of an aggressive medium in it and on the time to fracture at the same value of tensile stress was examined. Rods of various shapes of simply connected cross-section (circle, square and rectangles with different aspect ratios) provided that the areas of these sections are equal were studied [4]. In contrast to [3, 4], this article deals with two-connected cross-sections of rods, in which the area of the hollow (inner) part is 25% of the area of the bordering outer, loaded part. Also note that the shapes of the outer and inner contours of the cross sections are similar. The areas of the loaded parts of sections with different shapes coincide.

1. REVIEW OF MODERN WORKS ON THE INFLUENCE OF AN AGGRESSIVE MEDIUM ON THE DEFORMATION AND STRENGTH CHARACTERISTICS OF MATERIALS AND STRUCTURAL ELEMENTS, AND THEIR LONG-TERM FRACTURE

The study of the influence of an aggressive medium, which enters into both physical and chemical interaction with the material, taking into account phase transformations, was obtained by the authors [5–7]. The development of mechanical and mathematical models for describing the effect of mechanical stresses on the kinetics of chemical reactions in deformable bodies was considered. In this case, the physicochemical justification of the described approaches is taken into account, in particular, the equations of chemical reactions that occur at the interfaces between solid phases (metal, oxide) and gaseous substances are used. The models take into account the influence of external and internal stresses generated by chemical reactions. The influence of the type of stress state, magnitudes and signs of stress on the course of chemical reactions is investigated. The stability of the propagation of the chemical reaction front in a stressed body is investigated. The kinetics of the reaction front in the vicinity of stress concentrators and the relationship of chemical reactions with fracture processes are considered. Taking into account the chemical reaction localized at the reaction front in the “deformable body–gaseous component” system, the balance of mass, momentum, and energy is recorded, after which an expression for entropy production is derived, which allows one to naturally obtain a formula for the chemical affinity tensor, using which both the chemical equilibrium and the kinetics of the transformation front are determined.

Of particular interest is the study of the effect of ionizing radiation on the deformation and strength characteristics of materials and structural elements. Ionizing radiation can also be considered an aggressive medium that affects the physical and mechanical characteristics of the material subjected to its influence. This effect consists in the appearance of radiation defects in the crystal lattice of metals and the swelling of the metal (an increase in the volume of the metal when exposed to ionizing radiation). The article [8] considers the features of the methodology for constructing models of deformation and fracture of materials under radiation exposure using the theory of kinetic parameters [9], as well as models describing radiation deformations (swelling) of the material [10]. The results of experiments on the influence of the type and kind of stress state on radiation swelling and creep of materials are analyzed.

The review [11] shows that, depending on the type of materials, the radiation environments lead to different changes in the short-term and long-term mechanical characteristics of materials, as well as to radiation swelling. Experimental data on the effect of radiation exposure on the mechanical properties of steels and alloys (deformation curve, elastic modulus, yield strength, tensile strength, creep and creep rupture strength) are presented and analyzed. Special attention is paid to the presence of radiation swelling and the effect of the type of stress state on the creep and creep rupture strength of materials under radiation exposure.

It is recommended to take these effects into account when constructing models of deformation and destruction of materials and structures under radiation exposure [10]. The authors [10] note that radiation exposure leads to the need to take into account its effect on strength, plastic characteristics, and especially creep.

Earlier, for example, [12, 13], it was found that neutron irradiation, among other things, leads to an increase in the creep rate, a decrease in the creep rupture strength and plasticity of the material. Based on the analysis of experimental data, a model of intergranular fracture of austenitic steels is proposed, which takes into account the effect of neutron irradiation on creep rupture strength and ductility. The developed approaches are applicable for predicting the kinetics of crack propagation in time at various neutron flux intensities and taking into account the accumulated fluence.

Scientists from Nizhny Novgorod (Academician F.M. Mitenkov, Professor Yu.G. Korotkikh, etc.) made a great contribution to the development of experimental and theoretical research of the effect of ionizing radiation on stress–strain states and fracture processes. Mathematical models, algorithms and programs for calculating the processes of nonisothermal elastic–plastic deformation and accumulation of fatigue damage in the material of hazardous areas of equipment and systems of nuclear power plants were developed on the basis of modern achievements in the mechanics of damaged media (MDM) and fracture mechanics [14]. The developed models make it possible to take into account the effect on the rate of damage accumulation processes of multiaxial stress state, rotation of the principal planes of stress and strain tensors, and to take into account the nonlinear summation of damage when changing loading conditions.

The forecasting method in the study [15] is mainly based on the work of S. A. Shesterikov. The constants included in the basic equations are determined from the results of creep tests at three stress levels. Experimental data obtained during testing of 08H16N11M3-PD steel for creep and creep rupture strength at 600°C and 650°C are presented. Based on these data, the average theoretical values of the short-term strength limit and other coefficients of the basic equations are calculated. In the specified temperature

range, to predict the creep rupture strength of steel, taking into account its radiation exposure, the assumption is used that the ratio of the failure strain according on the tensile diagram to the failure strain during creep is equal for AISI 316 and 08H16N11M3-PD steels that are similar in composition. It was revealed that radiation exposure leads to a significant decrease in the creep rupture strength limit.

At the end of the theoretical part of the review, we note that various aspects of the influence of an aggressive environment on the characteristics of deformation and fracture of modern metals and alloys are considered in a large number of monographs (among them, for example, [16–18]).

So, for example, in the monograph [16], the deformation and destruction of the metal of the equipment of nuclear reactors under radiation and thermal effects are considered. Data on thermal and radiation creep are compared, and changes in the mechanical properties and swelling of the material under neutron irradiation are discussed. The influence of the cooling medium on the corrosion fatigue and stress corrosion of austenitic steel is considered. The features of cyclic deformation under neutron irradiation are analyzed. The corrosion growth of cracks under constant and cyclic loads is considered. The fracture criteria are given for various conditions of metal operation. The author provides a phenomenological description of experimental data for thermal and radiation creep. Kinetic equations for complex loading are proposed, as well as a method for calculating nonstationary problems of thermoplasticity. Recommendations for the practical use of the results obtained are given.

The monograph [17] examines the issues of modeling the behavior of reinforced concrete elements of structures under the influence of chloride-containing media, and the monograph [18] examines the performance of structures under conditions of high-temperature hydrogen corrosion.

Let us bring to the attention of the readers of this article some experimental works, among which we note a number of studies that were carried out at the Prometey Central Research Institute of Structural Materials (St. Petersburg) [19, 20]. The creep and creep rupture strength of materials and structural elements of equipment for nuclear power plants in contact with a liquid-metal aggressive medium were experimentally investigated.

The issues of creep rupture strength of structural materials operating in a reactor plant with a liquid-metal lead coolant have been studied [19]. The operating temperature of a lead-based liquid metal coolant exceeds 500°C, i.e., it is in the temperature range at which creep processes can occur intensively in steels. It is noted that the disadvantage of lead-based coolants is their aggressiveness towards structural materials; a measure to combat this aggressiveness is to maintain a certain concentration of oxygen in the liquid coolant. As a result, an oxide film forms on the surface of the steel, which prevents the material from contacting the liquid metal coolant. The experimental data obtained during long-term tests of samples of two grades of steel 10H15N9S3B and 10H9NSMFB are presented, namely, data on the creep rupture strength of these steel grades in air and in a stream of liquid lead are given. As a result, it was shown that the creep rupture strength of the samples tested in a flow of liquid lead is lower than the creep rupture strength of the samples tested in air. The reasons for the decrease in creep rupture strength in liquid lead were revealed in the course of metallographic analysis, which showed that at a high level of stress, there are traces of frontal liquid metal corrosion on the samples. With a decrease in the stress level, a dense oxide film is observed on the samples, the continuity of which is violated the more, the closer it is to the place of destruction of the sample. This film protects the sample from aggressive environmental influences, and its thickness depends on the level of stress and the duration of contact with the liquid metal.

The influence of liquid-metal lead coolant on the creep of chromium martensitic steel of grade 10H9NSMFB was studied [20]. When carrying out tests for creep rupture strength, an increased creep rate of steel in contact with liquid lead at a temperature of 550°C was noted in comparison with the creep rate in air. The article presents the results of experiments and their discussion, within the framework of which an explanation of the different behavior of the creep curves of samples tested in contact with liquid lead and in air at a stress level of 98 MPa and 68.6 MPa is given. It is stated that the data of metallographic analysis of samples destroyed in a flow of liquid lead indicate the presence of two fundamentally different mechanisms of destruction of samples in contact with a lead coolant. This phenomenon, discovered in [19], is associated with the influence of the stress level on the stability of oxide films. In conclusion, the authors note that in order to increase the reliability of a reactor plant with a liquid-metal coolant based on lead, when calculating the maximum permissible stresses in structures operating in contact with liquid lead, it is recommended to take into account the creep limits of structural materials, introducing restrictions on the allowable deformation on the selected time base.

In addition to studies describing the effect of a liquid metal medium on the long-term properties of steels, the employees of the Prometey Central Research Institute of Structural Materials carried out studies on the influence of this medium on the cyclic durability of materials.

Further, we note the work on the topic of the influence of an aggressive environment. The resistance of steel to stress corrosion in a corrosive environment (salt vapors) under slow tension was determined experimentally [21]. Review [22] considers the effect of neutron irradiation on the magnitude of mechanical stress that causes corrosion cracking. Published research results indicate that an increase in the dose of neutron radiation leads to a continuous decrease in the resistance of steel to stress-corrosion destruction. However, it has been shown that at the yield point, a certain saturation of its growth is observed with an increase in the radiation dose. Thus, the corrosion cracking limit does not correlate with the yield strength after irradiation.

The effect of irradiation on the fracture toughness is noted [23], which manifests itself in the shift of the fracture toughness curve to the region of higher temperatures after irradiation. The radiation swelling of two grades of austenitic chromium-nickel steel is investigated [24]. The dependence of the swelling of steels on the intensity of accumulated damage is shown and determined.

Low-temperature creep under the action of neutron irradiation is studied in [25].

The swelling of austenitic steel is considered in [26]. The temperature of maximum swelling and the swelling rate depend on the intensity of radiation damage. The swelling manifests itself after the accumulation of a certain threshold of radiation damage. This threshold value depends on the effective stress, temperature, and damage rate. Stretching and low-cycle fatigue of steel under neutron irradiation are studied in [27].

The effect of irradiation with Fe ions at 450°C is estimated [28] to study the cracking susceptibility of austenitic stainless steel 304L. After irradiation of 10 MeV Fe up to 5 dpa (dpa, displacements per atom), the irradiation-induced damage in the microstructure was characterized and quantified along with nano-hardness measurements. The material irradiated with Fe ions, strained to 4% in a light water medium in a pressurized water reactor (PWR), showed sites of crack nucleation that were similar to those found in neutron- and proton-irradiated materials. In comparison, the Fe-ion-irradiated material subjected to 4% plastic deformation in an inert argon atmosphere did not show any cracking, suggesting that localized deformation alone is insufficient to initiate cracking for the irradiation conditions used in this study.

The influence of mechanical treatment on the initiation of stress corrosion cracking of annealed stainless austenitic steel of type 316L in the primary water of a pressurized water reactor is considered [29]. This fact was investigated by accelerated testing in high temperature hydrogenated water. It was noted that stress corrosion cracks only occur on machined surfaces with machining notches perpendicular to the load direction, and a porous inner oxide layer was identified as an important factor contributing to cracking. In addition, most of the cracks ended up inside the near-surface ultrafine-grained layer caused by machining, and the residual stresses caused by machining, apparently, did not appear to have a significant effect on the occurrence of the crack. The correlation between crack nucleation and surface–near-surface elements is revealed and discussed.

The study [30] deals with the oxidation behavior of Zry-4 nuclear fuel cladding tubes in mixed steam–air atmospheres. Zry-4 oxidation tests were carried out at temperatures of 1373 and 1573 K. Measurement of the weight gain after the test, as well as the metallographic study, were carried out for a separate study of the kinetics of the region where nitrides are formed and the region free of nitrides. The results of oxidation tests at 1273 and 1473 K previously published by the same authors, are also discussed. The weight gain from the nitride-free region was estimated by a one-dimensional model of oxygen diffusion, using the finite-difference method, and the thickness of the metal part of the oxidized sample, columnar oxide, and oxygen-stabilized α -Zr(O), as well as the fraction of columnar oxide at the oxide–metal interface, were measured. The results show that nitrides are formed under a protective columnar oxide layer and that most of the mass gain associated with the formation of porous mixed regions of ZrN–ZrO₂ was associated with the formation of ZrO₂ from α -Zr (O).

The evolution of the microstructure after creep under irradiation in several austenitic steels irradiated to 120 dpa at 320°C is traced [31]. Tubes under pressure with stresses of 127–220 MPa were irradiated in fast reactor BOR-60 to 120 dpa at 320°C. The creep behavior depended on both the chemical composition and the metallurgical state of the steels. Various steels, irradiated and unloaded, were studied. Without mechanical stress, the irradiation resulted in a high density of dislocation lines and Frank loops and, depending on the type of steel, phase precipitation occurred. Mechanical stress caused an increase in the average size and density of the precipitated phase and, for some grades of steel, an increase in the average size of the loop and a decrease in their density. Anisotropy of the Frank loop density or size caused by mechanical stress has not been observed systematically. The microstructure of the dislocation line does not appear to differ between stressed and unstressed samples. No cavities were found in these samples. In comparison with the data of this work, the main models of irradiation creep are discussed.

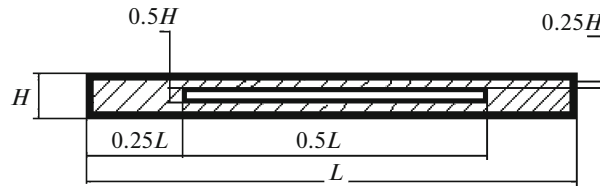


Fig. 1. Cross-section of a long rod in the form of a thin rectangle with a hole.

The character of creep under irradiation with heavy ions of annealed Cu films 200 nm and 500 nm thick was determined [32] and is characterized by the use of uniaxial microstretching test structures on the crystal. The tests were carried out at room temperature with an applied stress of 100 to 250 MPa and a damage accumulation rate of 5×10^{-4} and 6.3×10^{-4} dpa s^{-1} . The advantage of the method is that it allows simultaneous measurement of several tens of samples completely irradiated over their entire thickness. It was found that the plasticity mechanisms are noticeably more uniform during creep, taking into account radiation exposure, than under static load alone. The law of power-law creep includes a stress index equal to 5, which weakly depends on the microstructure of the films. Microstructural observations suggest that the creep mechanism is the result of dislocation sliding by means of their climb, which is explained by a simple closed-form model.

A brief review of the studies presented indicates the importance of taking into account the effect of an aggressive environment on the creep rupture strength of materials and structural elements.

2. PROBLEM STATEMENT

This article discusses three cross-sectional shapes of stretchable rods: a hollow rectangle with the lengths of one pair of sides many times less than the lengths of the other pair of sides, a hollow rectangle with the lengths of the sides of the same order, and a ring. To study the diffusion process in such rods, various variants of the diffusion equations are used: a one-dimensional equation in the first case, a two-dimensional equation in the second case, and an axisymmetric equation in the third case. In all three cases, zero initial conditions and constant values of the concentration of the aggressive medium on the contours of the cross sections are taken. Exact solutions of the diffusion equation can only be represented as infinite series. In this article, approximate equations are considered, while the initial and boundary conditions are satisfied exactly, and the equation itself is satisfied integrally.

To analyze the dependence of the diffusion process of an aggressive environment on the contour of the cross-section of the rod, an approximate method for solving the diffusion equation is used, based on the introduction of a diffusion front, propagating from the surface of the rod [33–35]. This approach allows one to divide all the material of the cross-section of the rod into a perturbed region (in which the medium has already penetrated into the material) and an unperturbed region (in which there is no penetration of the medium yet) and then track the movement of the boundary between these regions in time.

3. ONE-DIMENSIONAL DIFFUSION EQUATION IN CARTESIAN COORDINATES

Consider a long rod with a cross-section in the form of a thin rectangle with sides L and H ($L \gg H$) (Fig. 1).

We select from the middle part of this rectangle a rectangular hole with sides $L/2$ and $H/2$, i.e., the area of the hole is 25% of the area of the outer rectangle. As a result, the cross-section of the original rectangle consists of two rectangles with sides $L/4$ and H (Fig. 1) and two rectangles with sides $L/2$ and $H/4$ (Fig. 1). Since the lengths of all the considered rectangles significantly exceed their heights, then in all these rectangles the diffusion process of the introduction of environmental elements into the material of the rod can be considered as one-dimensional (the influence of an aggressive medium into the rod from the short sides of its section can be neglected).

Consider the diffusion process in each of these rectangles. For the concentration c of the medium in the rod material, we take a zero initial value, and the equality of the concentration c to the constant value c_0 is used as the boundary condition on the surfaces of the wide sides of the cross-section of the rod.

We introduce dimensionless variables

$$\bar{y} = \frac{2y}{H}, \quad \bar{t} = \frac{48D}{H^2}t, \quad \bar{c} = \frac{c}{c_0},$$

where y is the transverse coordinate along the thickness of the rectangular element under consideration ($y = 0$ is in the middle of the cross section), t is the time, c is the concentration, c_0 is the constant concentration at the boundary of the rod material and the external environment, and D is the diffusion coefficient. From the symmetry condition, we consider half of the cross-section of a rectangular element in thickness. The one-dimensional diffusion equation [36, 37] in these variables takes the following form:

$$\frac{\partial \bar{c}}{\partial \bar{t}} = \frac{1}{12} \frac{\partial^2 \bar{c}}{\partial \bar{y}^2}, \quad 0 \leq \bar{t} < \infty, \quad 0 < \bar{y} < 1. \quad (3.1)$$

The initial and boundary conditions, due to the symmetry of the diffusion process, relative to the middle of the rod, are written as:

$$\bar{c}(\bar{y}, 0) = 0, \quad \bar{c}(1, \bar{t}) = 1, \quad \frac{\partial \bar{c}}{\partial \bar{y}}(0, \bar{t}) = 0.$$

We use an approximate method for solving the diffusion equation (3.1), based on the introduction of a diffusion front [35].

In this work, the dependence of the concentration \bar{c} on the coordinate \bar{y} is taken in the form of a square polynomial satisfying the boundary and initial conditions. In this case, two stages of the diffusion process are considered: the stage of front penetration and the stage of saturation, which are separated by the moment of time \bar{t}_0 [33, 35].

$$\bar{c}(\bar{y}, \bar{t}) = \begin{cases} 0 & \text{when } 0 \leq \bar{y} \leq \bar{l}(\bar{t}) \\ \{1 - [(1 - \bar{y}) / (1 - \bar{l})]\}^2 & \text{when } \bar{l}(\bar{t}) < \bar{y} \leq 1 \end{cases} \quad \text{when } 0 < \bar{t} \leq \bar{t}_0 \quad (3.2)$$

$$\bar{c}(\bar{y}, \bar{t}) = B + [1 - B](\bar{y})^2 \quad \text{when } \bar{t} > \bar{t}_0,$$

where $\bar{l}(\bar{t})$ is the coordinate of the diffusion front, \bar{t}_0 is the transition time between stages of the diffusion process, and $B = B(\bar{t})$ is the concentration in the center of the cross-section of the rod at $\bar{t} \geq \bar{t}_0$ (at the midline $\bar{y} = 0$).

The unknown dependences of $\bar{l}(\bar{t})$ and $B(\bar{t})$ are determined from the integral satisfaction of the parabolic function $\bar{c}(\bar{y}, \bar{t})$ by (3.2) to the diffusion equation (3.1)

$$\int_0^1 \left| \frac{\partial \bar{c}}{\partial \bar{t}} - \frac{1}{12} \frac{\partial^2 \bar{c}}{\partial \bar{z}^2} \right| d\bar{z} = 0. \quad (3.3)$$

It is shown [35] that if the sign of the module of the integrand is excluded in (3.3), then the difference between the obtained approximate solution of the diffusion equation and the exact solution is only a few percent; therefore, further, when using Eq. (3.3), we omit the sign of the modulus.

Substituting (3.2) into (3.3), we obtain the coordinate of the diffusion front $\bar{l}(\bar{t})$ and the concentration $B(\bar{t})$ in the following form

$$\bar{l} = 1 - \sqrt{\bar{t}}, \quad B = 1 - \exp\left(-\frac{\bar{t} - \bar{t}_0}{4}\right). \quad (3.4)$$

The diffusion front reaches the midline of the cross-section of the rod at time \bar{t}_0 , while $\bar{l} = 0$. Based on this boundary condition, we obtain the value of time $\bar{t}_0 = 1$.

Using relations for concentration (3.2) and relations (3.4), we obtain expressions for $\bar{c}(\bar{y}, \bar{t})$ in the following form

$$\bar{c}(\bar{y}, \bar{t}) = \begin{cases} \left[1 - \frac{1 - \bar{y}}{\sqrt{\bar{t}}} \right]^2 & \text{when } 1 - \sqrt{\bar{t}} < \bar{y} \leq 1 \\ 0 & \text{when } 0 \leq \bar{y} \leq 1 - \sqrt{\bar{t}} \end{cases} \quad \text{when } 0 < \bar{t} \leq 1,$$

$$\bar{c}(\bar{y}, \bar{t}) = 1 - (1 - \bar{y}^2) \exp\left[-\frac{1}{4}(\bar{t} - 1)\right] \quad \text{when } \bar{t} > 1.$$

In the future, to analyze the influence of an aggressive medium on the time to fracture of the rod, the integral average concentration $\bar{c}_m(\bar{t})$ will be used, which has the form

$$\bar{c}_m(\bar{t}) = \int_0^1 \bar{c}(\bar{y}, \bar{t}) d\bar{y} = \begin{cases} \frac{1}{3}\sqrt{\bar{t}}, & \text{when } 0 < \bar{t} \leq 1, \\ 1 - \frac{2}{3} \exp\left[-\frac{1}{4}(\bar{t} - 1)\right], & \text{when } \bar{t} > 1. \end{cases} \quad (3.5)$$

Here, expression (3.5) takes into account two stages of the diffusion process. At the first stage, at $0 \leq \bar{t} \leq 1$, the external medium penetrates into the material, which is characterized by the movement of the diffusion front. At the second stage, at $\bar{t} \geq 1$ at all points of the considered cross-section, the concentration is different from zero and it grows to full saturation.

Hence, in the case of a rectangle with sides H and $L/4$, we get:

$$\bar{c}_{m1}(t) = \begin{cases} G_1(t) = \frac{1}{3} \frac{\sqrt{48D}}{H} \sqrt{t}, & \text{when } 0 \leq t \leq \frac{H^2}{768D}, \\ G_2(t) = \frac{1}{3} \frac{\sqrt{48D}}{H} \sqrt{t}, & \text{when } \frac{H^2}{768D} \leq t \leq \frac{H^2}{48D}, \\ G_3(t) = 1 - \frac{2}{3} \exp\left[-\frac{1}{4}\left(\frac{48D}{H^2}t - 1\right)\right], & \text{when } t > \frac{H^2}{48D}. \end{cases} \quad (3.6)$$

Similarly, in the case of a long rectangle with sides $L/2$ and $H/4$ ($\bar{t} = \frac{768D}{H^2}t$), we have

$$\bar{c}_{m2}(t) = \begin{cases} G_4(t) = \frac{1}{3} \frac{\sqrt{768D}}{H} \sqrt{t}, & \text{when } 0 \leq t \leq \frac{H^2}{768D}, \\ G_5(t) = 1 - \frac{2}{3} \exp\left[-\frac{1}{4}\left(\frac{768D}{H^2}t - 1\right)\right], & \text{when } t > \frac{H^2}{768D}. \end{cases} \quad (3.7)$$

The dependence of the integrally averaged concentration level of an aggressive medium in the entire cross section of the original rectangle with a hole has the form

$$\bar{c}_m(t) = \frac{2}{3}\bar{c}_{m1}(t) + \frac{1}{3}\bar{c}_{m2}(t), \quad (3.8)$$

where $\bar{c}_{m1}(t)$ and $\bar{c}_{m2}(t)$ are determined by expressions (3.6) and (3.7), respectively.

Thus, the expression for the integrally averaged concentration of the considered cross-section has the form:

$$\bar{c}_m(t) = \begin{cases} \frac{2}{3}G_1(t) + \frac{1}{3}G_4(t), & \text{when } 0 \leq t \leq \frac{H^2}{768D}, \\ \frac{2}{3}G_2(t) + \frac{1}{3}G_5(t), & \text{when } \frac{H^2}{768D} \leq t \leq \frac{H^2}{48D}, \\ \frac{2}{3}G_3(t) + \frac{1}{3}G_5(t), & \text{when } t > \frac{H^2}{48D}. \end{cases} \quad (3.9)$$

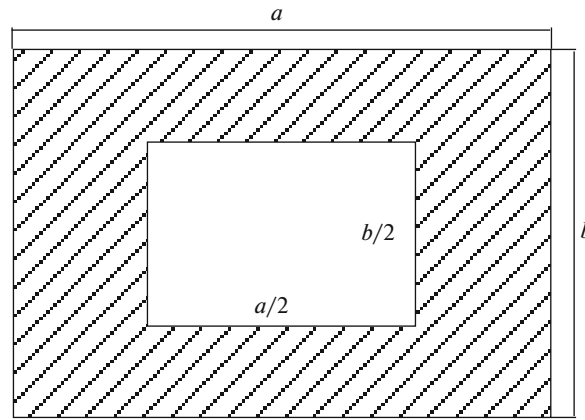


Fig. 2. Dimensions of the cross-section in the form of a hollow rectangle.

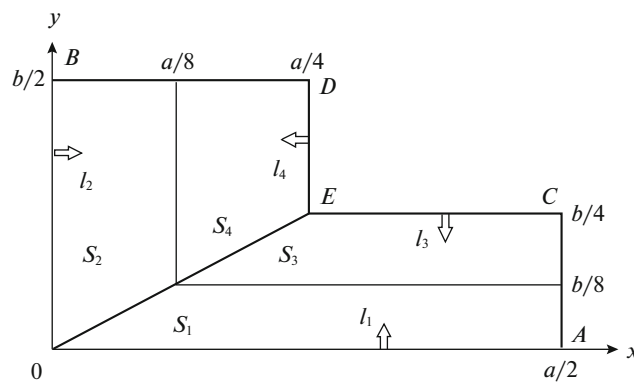


Fig. 3. A quarter section of a two-connected rectangle with a rectangular hole.

Since the area of the real cross-section F_{real} (cross-sectional area without a hole) is $F_{\text{real}} = 3/4F$, then taking into account the relations $F = HL$ and $\beta = H/L$, we get $H^2 = \beta F = 4/3\beta F_{\text{real}}$. Expression (3.9) will take the following form:

$$\bar{c}_m(t) = \begin{cases} \frac{2}{3}G_1(t) + \frac{1}{3}G_4(t), & \text{when } 0 \leq t \leq \frac{\beta F_{\text{real}}}{576D}, \\ \frac{2}{3}G_2(t) + \frac{1}{3}G_5(t), & \text{when } \frac{\beta F_{\text{real}}}{576D} \leq t \leq \frac{\beta F_{\text{real}}}{36D}, \\ \frac{2}{3}G_3(t) + \frac{1}{3}G_5(t), & \text{when } t > \frac{\beta F_{\text{real}}}{36D}. \end{cases} \quad (3.10)$$

4. TWO-DIMENSIONAL DIFFUSION EQUATION IN CARTESIAN COORDINATES

Consider the cross-section of a long rod in the form of a rectangle with sides a and b ($b/a = \alpha$), from which the inner part with sides $a/2$ and $b/2$ has been removed. From the symmetry condition, Fig. 2 shows a quarter of the cross-section under consideration: $0 \leq x \leq a/2$, $0 \leq y \leq b/2$, except for points whose coordinates satisfy two inequalities simultaneously: $a \leq 4x \leq 2a$ and $b \leq 4y \leq 2b$. Thus, the area of the hole inside the cross-section of the rod is 25% of the area of the full cross-section. The two-connected cross-section in question is located in an aggressive environment.

In the cross-sectional area S (S is the area of the considered quarter of the cross-section of a two-connected rectangle with a rectangular hole), we distinguish four components (Fig. 3):

$$\begin{aligned}
 S &= S_1 + S_2 + S_3 + S_4, \\
 S_1 : \quad &0 \leq y \leq l_1(t), \quad 2\frac{y}{\alpha} \leq 2x \leq a, \\
 S_2 : \quad &0 \leq x \leq l_2(t), \quad 2\alpha x \leq 2y \leq b, \\
 S_3 : \quad &4l_3(t) \leq 4y \leq b, \quad 2\frac{y}{\alpha} \leq 2x \leq a, \\
 S_4 : \quad &4l_4(t) \leq 4x \leq a, \quad 2\alpha x \leq 2y \leq b.
 \end{aligned}
 \tag{4.1}$$

Areas $(S_1 + S_3)$ and $(S_2 + S_4)$ are separated by OE .

To determine the concentration of an aggressive medium $c(x, y, t)$ in the cross-section under consideration, we use the well-known diffusion equation in Cartesian coordinates:

$$\frac{\partial c}{\partial t} - D \left(\frac{\partial^2 c}{\partial x^2} + \frac{\partial^2 c}{\partial y^2} \right) = 0.
 \tag{4.2}$$

As the initial concentration value in the considered cross-section of a two-connected rectangle with a rectangular hole ($OACEDBO$ polygon), we take the zero value

$$c(x, y, 0)|_S = 0.
 \tag{4.3}$$

Let us take as boundary values

$$\begin{aligned}
 c|_{OA} &= c|_{OB} = c|_{EC} = c|_{ED} = c_0, \\
 \frac{\partial c}{\partial x}|_{AC} &= \frac{\partial c}{\partial y}|_{BD} = 0.
 \end{aligned}
 \tag{4.4}$$

Similarly to [38], consider the derivation of an approximate solution of the diffusion equation (4.2) in the area S with initial (4.3) and boundary (4.4) conditions in the form of a second-degree polynomial in spatial coordinates with time-dependent coefficients. In obtaining this solution, the initial (4.3) and boundary (4.4) conditions are satisfied exactly, and the differential equation (4.2) itself is integral in the domain S . By analogy with Section 3, two stages of the diffusion process are considered. At the first stage, it is assumed that diffusion fronts $l_1(t)$ and $l_3(t)$, respectively, move in the regions S_1 and S_3 perpendicular to the Ox axis from the boundaries OA and EC into the cross-section, dividing the region $(S_1 + S_3)$ into unperturbed and perturbed parts. At $t = t_{01}$, the fronts $l_1(t)$ and $l_3(t)$ are connected: $l_1(t_{01}) + l_3(t_{01}) = b/4$. Similarly to the regions S_1 and S_3 in the regions S_2 and S_4 at the first stage, the diffusion fronts $l_2(t)$ and $l_4(t)$, respectively, move perpendicular to the Oy axis from the boundaries OB and ED into the cross-section, dividing the region $(S_2 + S_4)$ into unperturbed and perturbed parts. In the domain $(S_2 + S_4)$, at $t = t_{02}$, the equality $l_2(t_{02}) + l_4(t_{02}) = a/4$ holds. It can be shown that $t_{01} = t_{02} = t_0$. Throughout what follows, l_1, \dots, l_4 is understood as the coordinates of the corresponding fronts in the Ox and Oy axes. At $t > t_0$, the second stage of the diffusion process is realized in the $OACEDBO$ polygon.

4.1. The first stage of the diffusion process

The solution of the differential equation (4.2) is considered in this form:

$$c = \begin{cases} c_1(y, t) & \text{in } S_1, \\ c_2(x, t) & \text{in } S_2, \\ c_3(y, t) & \text{in } S_3, \\ c_4(x, t) & \text{in } S_4, \\ 0 & \text{in } (S_2 + S_4) \quad \text{when } l_2(t) \leq x \leq \frac{a}{4} - l_4(t), \\ 0 & \text{in } (S_1 + S_3) \quad \text{when } l_1(t) \leq y \leq \frac{b}{4} - l_3(t). \end{cases}
 \tag{4.5}$$

where

$$c_1(y, t) = c_0 \left(1 - \frac{y}{l_1}\right)^2, \quad c_2(x, t) = c_0 \left(1 - \frac{x}{l_2}\right)^2$$

$$c_3(y, t) = c_0 \left[1 - \frac{b - 4y}{b - 4l_3}\right]^2, \quad c_4(x, t) = c_0 \left[1 - \frac{a - 4x}{a - 4l_4}\right]^2$$

It is easy to show that the proposed version (4.5) of an approximate solution of Eq. (4.2) satisfies the conditions (4.3) and (4.4). To simplify the calculations, we introduce two hypotheses. First, let us assume that in $(S_1 + S_3)$ the speeds of the fronts $l_1(t)$ and $l_3(t)$ are equal in absolute value, i.e., $l_1(t) + l_3(t) = b/4$, similar to $l_2(t) + l_4(t) = a/4$. Second, let us assume that the speeds of the fronts from the outer surface of the cross-section are proportional to the lengths of the corresponding sides of the cross-section, i.e.,

$$\frac{l_2(t)}{l_1(t)} = \alpha = \text{const.}$$

As a result, the values of all four considered fronts $l_1(t) - l_4(t)$ can be reduced to one definable function $l_1(t)$:

$$l_1(t) = \alpha l_2(t), \quad l_3(t) = \frac{b}{4} - l_1(t), \quad l_4(t) = \frac{a}{4} - \alpha l_1(t). \quad (4.6)$$

When substituting the relations (4.5) in (4.2) and with additional allowance for (4.6), we obtain (hereinafter, the notation in the formulas “...” means that we omit the intermediate calculations):

$$\frac{1}{2c_0} \int_{S_1} \left[\frac{\partial c}{\partial t} - D \left(\frac{\partial^2 c}{\partial x^2} + \frac{\partial^2 c}{\partial y^2} \right) \right] dx dy = \dots = \frac{(b - l_1) \dot{l}_1}{12\alpha} - \frac{D(b - l_1)}{2\alpha l_1},$$

$$\frac{1}{2c_0} \int_{S_2} \left[\frac{\partial c}{\partial t} - D \left(\frac{\partial^2 c}{\partial x^2} + \frac{\partial^2 c}{\partial y^2} \right) \right] dx dy = \dots = \frac{(b - l_1) \dot{l}_1}{12\alpha} - \frac{D\alpha(b - l_1)}{2l_1},$$

$$\frac{1}{2c_0} \int_{S_3} \left[\frac{\partial c}{\partial t} - D \left(\frac{\partial^2 c}{\partial x^2} + \frac{\partial^2 c}{\partial y^2} \right) \right] dx dy = \dots = -\frac{(b + 2l_1) \dot{l}_1}{24\alpha} - \frac{(b + 2l_1) D}{4\alpha l_1},$$

$$\frac{1}{2c_0} \int_{S_4} \left[\frac{\partial c}{\partial t} - D \left(\frac{\partial^2 c}{\partial x^2} + \frac{\partial^2 c}{\partial y^2} \right) \right] dx dy = \dots = -\frac{(b + 2l_1) \dot{l}_1}{24\alpha} - \frac{(b + 2l_1) D\alpha}{4l_1}.$$

Substituting the resulting expressions into the equation

$$\int_S \left[\frac{\partial c}{\partial t} - D \left(\frac{\partial^2 c}{\partial x^2} + \frac{\partial^2 c}{\partial y^2} \right) \right] dx dy = 0,$$

where

$$S = S_1 + S_2 + S_3 + S_4,$$

we obtain:

$$\dot{l}_1 = \frac{9b(1 + \alpha^2)}{(b - 4l_1)l_1} D. \quad (4.7)$$

We introduce the variables: $\hat{l}_1 = l_1/b$, $\hat{D} = D/b^2$, then Eq. (4.7) for determining the dependence of the coordinate of the diffusion front on time will be written in the form

$$(1 - 4\hat{l}_1)\hat{l}_1 \frac{d\hat{l}_1}{dt} = 9(1 + \alpha^2)\hat{D}. \quad (4.8)$$

Since at the initial moment of time $t = 0$, $\hat{l}_1 = 0$, i.e., the derivative $d\hat{l}_1/dt$ is infinite, we pass in Eq. (4.8) to the inverse function and obtain the solution of the initial problem $t(\hat{l}_1 = 0) = 0$ in the form

$$t = K \left(\frac{\hat{l}_1^2}{2} - \frac{4}{3} \hat{l}_1^3 \right).$$

The symmetry condition implies:

$$t_0 = t \left(\hat{l}_1 = \frac{1}{8} \right) = \frac{K}{192}. \tag{4.9}$$

Next, we will calculate the integrally averaged concentration of the aggressive medium in the rod material during the first stage of the diffusion process. The quarter-section area of a two- connected rectangle with a rectangular hole is $\frac{3}{16} ab$.

$$\frac{3}{16} ab \bar{c}_m(t) = I_1 + I_2 + I_3 + I_4, \tag{4.10}$$

where,

$$\begin{aligned} I_1 &= \int_0^{\hat{l}_1} \left(\frac{a}{2} - \frac{y}{\alpha} \right) \left(1 - \frac{y}{\hat{l}_1} \right)^2 dy = \frac{ab}{12} (2\hat{l}_1 - \hat{l}_1^2), \\ I_2 &= \int_0^{\hat{l}_2} \left(\frac{b}{2} - \alpha x \right) \left(1 - \frac{x}{\hat{l}_2} \right)^2 dx = \frac{ab}{12} (2\hat{l}_1 - \hat{l}_1^2), \\ I_3 &= \int_{\hat{l}_3}^{b/4} dy \int_{y/\alpha}^{a/2} \left(1 - \frac{b-4y}{b-4\hat{l}_3} \right)^2 dx = \frac{abl_1}{12} + \frac{abl_1^2}{12}, \\ I_4 &= \int_{\hat{l}_4}^{a/4} \left(\frac{b}{2} - \alpha x \right) \cdot \left(1 - \frac{a-4x}{a-4\hat{l}_4} \right)^2 dx = \dots = \frac{ab\hat{l}_1}{12} + \frac{ab\hat{l}_1^2}{12}. \end{aligned}$$

Substituting $I_1 - I_4$ in (4.10), we obtain $\bar{c}_m(t) = \frac{8}{3} \hat{l}_1$. Then, given the solution (4.9) for the moment of time $t_0 = t(\hat{l}_1 = 1/8)$, we obtain

$$K_2 = \frac{b^2}{9(1 + \alpha^2)D}, \quad t_0 = t \left(\frac{\hat{l}_1}{b} = \frac{1}{8} \right) = \frac{1}{512} K_2, \quad \bar{c}_m(t_0) = \frac{1}{3}.$$

4.2. The Second Stage of the Diffusion Process

At $t > t_0$, the second stage of the diffusion process begins; at any point of the considered cross-section, the concentration of the aggressive medium $c(x, y, t)$ is positive, while it increases with time. The boundary conditions at the boundaries of the section OA, OB, EC, ED are still characterized by a constant value of $c = c_0$, along the segment $AC: \frac{\partial c}{\partial x}(a/2, y, t) = 0$, along the segment $BD: \frac{\partial c}{\partial y}(x, b/2, t) = 0$, the initial values in the regions $S_1 \dots S_4$ coincide with the corresponding functions $c(x, y, t_0)$ at the end of the first stage. As before, we will use the dimensionless concentration $\bar{c} = c/c_0$. At the end of the first stage, the concentration in the regions $(S_1 + S_3)$ represents the parabolic dependence of \bar{c} on y

$$\bar{c}(x, y, t_0) = \left(1 - 8 \frac{y}{b} \right)^2$$

with zero $\bar{c} = 0$ along the segment $y = b/8$. Suppose that in these regions the dependence of the concentration \bar{c} on the y coordinate is still described by a quadratic parabola, in which the minimum value of \bar{c} , equal to $B_1(t)$, is realized at $y = b/8: \bar{c}(x, b/8, t) = B_1(t)$.

Let us represent the expression for the concentration $\bar{c}(x, y, t_0)$ in the regions $(S_1 + S_3)$ in the following form

$$\bar{c}(x, y, t_0) = 1 - 16(1 - B_1) \frac{y}{b} + 64(1 - B_1)^2 \left(\frac{y}{b}\right)^2. \quad (4.11)$$

It is obvious that the relation (4.11) satisfies all the initial and boundary conditions in the exact formulation. Substituting (4.11) into the diffusion equation (4.2), we obtain:

$$\left(1 - \frac{4}{b}y^2\right) \dot{B}_1 = \frac{8}{b}D(1 - B_1).$$

Let us write down the integral consequence of the diffusion equation in the domains ($S_1 + S_4$):

$$\int_{(S_2+S_4)} \left[\frac{\partial \bar{c}}{\partial t} - D \left(\frac{\partial^2 \bar{c}}{\partial x^2} + \frac{\partial^2 \bar{c}}{\partial y^2} \right) \right] dx dy = \frac{ab}{16} \dot{B}_1 - D \frac{12a}{b} (1 - B_1). \quad (4.12)$$

Let us represent a similar dependence of $\bar{c}(x, y, t)$ in the region ($S_2 + S_4$) in the form:

$$\bar{c}(x, y, t) = 1 - \frac{16}{a}(1 - B_2)x + \frac{64}{a^2}(1 - B_2)x^2.$$

It is easy to show that this expression for $\bar{c}(x, y, t_0)$ in the region ($S_2 + S_4$) at $t = t_0$ satisfies all the initial and boundary conditions. The derivatives used take the following form:

$$\int_{(S_2+S_4)} \left[\frac{\partial \bar{c}}{\partial t} - D \left(\frac{\partial^2 \bar{c}}{\partial x^2} + \frac{\partial^2 \bar{c}}{\partial y^2} \right) \right] dx dy = \frac{ab}{16} \dot{B}_2 - D \frac{12b}{a} (1 - B_2). \quad (4.13)$$

It can be shown that $B_1(t) = B_2(t) = B(t)$. Adding (4.12) and (4.13), we obtain an integral consequence of the diffusion equation in the form:

$$\dot{B} = K_1(1 - B)D,$$

where

$$K_1 = \frac{96}{b^2}(\alpha^2 + 1)D = \frac{96}{\alpha F}(\alpha^2 + 1)D.$$

Its solution for the initial data $B(t_0) = 0$ has the form:

$$B(t) = 1 - \exp[-K_1(t - t_0)].$$

Let us calculate the concentration of the aggressive medium, integrally averaged over the rod material, in the second stage of the diffusion process. We have

in the range

$$(S_1 + S_3): \bar{c}(x, y, t) = 1 - 16 \left[1 - 4 \frac{y}{b} \right] \frac{y}{b} \exp[-K_1(t - t_0)]$$

in the range

$$(S_2 + S_4): \bar{c}(x, y, t) = 1 - 16 \left[1 - 4 \frac{x}{a} \right] \frac{x}{a} \exp[-K_1(t - t_0)].$$

From here we obtain the average value:

$$\bar{c}_m(t) = 1 - \frac{2}{3} \exp \left[-\frac{96}{\alpha F} (\alpha^2 + 1) D (t - t_0) \right]. \quad (4.14)$$

5. THE DIFFUSION EQUATION IN AN AXISYMMETRIC FORMULATION

In this section, we consider the axisymmetric problem of the diffusion of environmental elements into a hollow rod, the cross-section of which has the shape of a ring. The outer radius of the ring is R and the inner radius is $R/2$, and the cross-sectional area of the hollow hole in the rod is 25 percent of the total cross-sectional area of the rod (Fig. 4).

As before, we will consider the zero initial condition for the concentration, and as the boundary condition on the surfaces of the rod, we will take the condition that the concentration c is equal to the constant value c_0 . We introduce the dimensionless variables

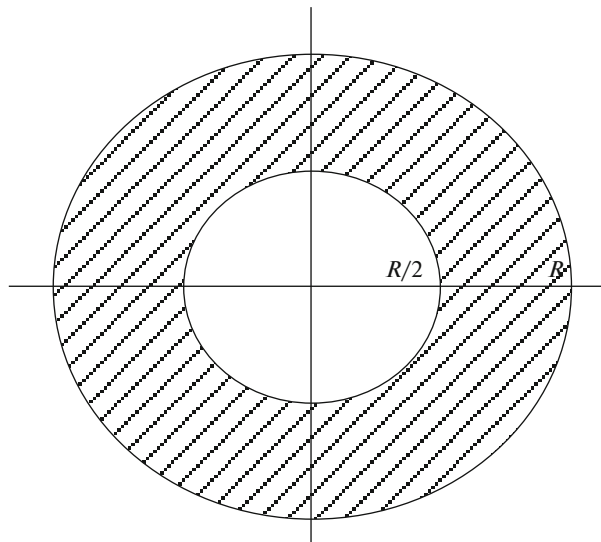


Fig. 4. Dimensions of the cross-section in the form of a ring.

$$\tilde{r} = \frac{r}{R}, \quad \tilde{t} = \frac{D_0}{R^2} t,$$

in which the diffusion equation takes the form:

$$\frac{\partial \bar{c}(\tilde{r}, \tilde{t})}{\partial \tilde{t}} = \frac{1}{\tilde{r}} \frac{\partial}{\partial \tilde{r}} \left(\tilde{r} \frac{\partial \bar{c}}{\partial \tilde{r}} \right), \quad \bar{c}(\tilde{r}, 0) = 0, \quad \bar{c}(1, \tilde{t}) = 1, \quad \bar{c}(1/2, \tilde{t}) = 1.$$

Consider the first stage of the diffusion process. Dependences of concentration on the coordinate and time are given as polynomials of the second degree in the coordinate. The indicated dependences take into account the time-dependent coordinates of two diffusion fronts moving from the inner and outer sides of the cross-section of the rod in the form of a ring.

$$\bar{c}(\tilde{r}, \tilde{t}) = \begin{cases} \left[\frac{\tilde{r} - \tilde{l}_1}{1/2 - \tilde{l}_1} \right]^2, & \text{when } 1/2 \leq \tilde{r} \leq \tilde{l}_1(\tilde{t}), \quad 0 < \tilde{t} \leq \tilde{t}_0, \\ 0, & \text{when } \tilde{l}_1(\tilde{t}) \leq \tilde{r} \leq \tilde{l}_2(\tilde{t}), \quad 0 < \tilde{t} \leq \tilde{t}_0, \\ \left[\frac{\tilde{r} - \tilde{l}_2}{1 - \tilde{l}_2} \right]^2, & \text{when } 1 \leq \tilde{r} \leq \tilde{l}_2(\tilde{t}), \quad 0 < \tilde{t} \leq \tilde{t}_0, \end{cases} \quad (5.1)$$

where $\tilde{l}_1(\tilde{t})$, and $\tilde{l}_2(\tilde{t})$ are the coordinates of diffusion fronts from the inner and outer sides of the ring, respectively.

Let us define the functions $\tilde{l}_1(\tilde{t})$ and $\tilde{l}_2(\tilde{t})$ from the integral consequences of the diffusion equation and the diffusion equation with weight \tilde{r} :

$$\int_{1/2}^1 \left[\frac{\partial \bar{c}}{\partial \tilde{t}} - \frac{1}{\tilde{r}} \frac{\partial}{\partial \tilde{r}} \left(\tilde{r} \frac{\partial \bar{c}}{\partial \tilde{r}} \right) \right] \tilde{r} d\tilde{r} = 0, \quad \int_{1/2}^1 \left[\frac{\partial \bar{c}}{\partial \tilde{t}} - \frac{1}{\tilde{r}} \frac{\partial}{\partial \tilde{r}} \left(\tilde{r} \frac{\partial \bar{c}}{\partial \tilde{r}} \right) \right] \tilde{r}^2 d\tilde{r} = 0$$

As a result, we obtain a system of differential equations

$$\begin{aligned} \frac{1 + \tilde{l}_1}{12} \dot{\tilde{l}}_1 - \frac{1 + \tilde{l}_2}{6} \dot{\tilde{l}}_2 &= \frac{2\tilde{l}_1 + 1}{2\tilde{l}_1 - 1} + \frac{\tilde{l}_2 + 1}{1 - \tilde{l}_2} \\ \frac{12\tilde{l}_1^2 + 8\tilde{l}_1 + 3}{12} \dot{\tilde{l}}_1 - \frac{\tilde{l}_2^2 + \tilde{l}_2 + 4}{10} \dot{\tilde{l}}_2 &= \frac{2\tilde{l}_1^2 + \tilde{l}_1 + 2}{2\tilde{l}_1 - 1} + \frac{\tilde{l}_2^2 + \tilde{l}_2 + 4}{1 - \tilde{l}_2} \end{aligned} \quad (5.2)$$

with initial conditions $\tilde{l}_1(0) = 1/2$, and $\tilde{l}_2(0) = 1$.

The dependences $\tilde{l}_1(\tilde{t})$, and $\tilde{l}_2(\tilde{t})$ were found from system (5.2) numerically. These, in turn, were used to determine the dependence of the concentration on the coordinate and time $\bar{c}(\tilde{r}, \tilde{t})$.

At the beginning of the second stage of the diffusion process, the concentration in the entire rod is non-zero and is determined at the end of the first stage when two diffusion fronts join. The dependence of concentration on time is given in the form

$$\bar{c}(\tilde{r}, \tilde{t}) = \begin{cases} B + (1 - B) \left[\frac{\tilde{r} - \tilde{l}}{1/2 - \tilde{l}} \right]^2, & \text{when } 1/2 \leq \tilde{r} \leq \tilde{l}(\tilde{t}), \quad \tilde{t} > \tilde{t}_0, \\ B + (1 - B) \left[\frac{\tilde{r} - \tilde{l}}{1 - \tilde{l}} \right]^2, & \text{when } \tilde{l}(\tilde{t}) \leq \tilde{r} \leq 1, \quad \tilde{t} > \tilde{t}_0, \end{cases} \quad (5.3)$$

where $\tilde{l}(\tilde{t})$ is the coordinate of the junction point of the fronts at the end of the first stage of the diffusion process, corresponds to the minimum concentration over the cross-section of the hollow rod, and $B(\tilde{t})$ is the concentration at the specified junction point of the fronts.

Carrying out the reasoning and calculations similar to those carried out in the first stage, we obtain the following system of differential equations.

$$\begin{aligned} \frac{(4\tilde{l} + 9)}{48} \dot{B} + \left[\frac{\dot{\tilde{l}}}{12} - \frac{2\tilde{l}}{(\tilde{l} - 1)(2\tilde{l} - 1)} \right] (B - 1) &= 0, \\ \frac{(4\tilde{l}^2 + 9\tilde{l} + 14)}{40} \dot{B} + \left[\frac{\dot{\tilde{l}}(8\tilde{l} + 9)}{40} + \frac{2(\tilde{l}^2 + 3\tilde{l} - 1)}{(1 - 2\tilde{l})(\tilde{l} - 1)} \right] (B - 1) &= 0. \end{aligned} \quad (5.4)$$

The initial conditions of system (5.4) are as follows:

$$\tilde{l}(\tilde{t}_0) = 0.88, \quad \text{and} \quad B(\tilde{t}_0) = 0.$$

The value of the right part of the first initial condition is assumed to be equal to the value of the solution of the system (5.2) at time $\tilde{t}_0 = 0.002$ of the end of the first stage of the diffusion process. The second initial condition means the concentration value at the point of closing of the fronts at the end of the first stage of the diffusion process at time \tilde{t}_0 . As for the first stage, the dependence $B(\tilde{t})$, and $\tilde{l}(\tilde{t})$ were determined from the numerical solution of the system (5.4).

The integrally averaged concentration is determined by the expression:

$$\bar{c}_m(t) = \frac{1}{F_c} \int_{R/2}^R \bar{c}(r, t) r dr,$$

where $F_c = 0.75\pi R^2$ is the cross-sectional area of the rod in the form of a ring.

6. CREEP RUPTURE STRENGTH OF THE STRETCHED RODS IN AN AGGRESSIVE ENVIRONMENT

Let us consider a kinetic equation in which the rate of damage accumulation depends on the tensile stress σ_0 (which takes the same value in all the considered rods) and on the integrally averaged concentration level of the aggressive medium \bar{c}_m in the following form [9]:

$$\frac{d\omega}{dt} = A \left(\frac{\sigma_0}{1 - \omega(t)} \right)^n f(\bar{c}_m(t)), \quad \omega(0) = 0, \quad \omega(t^*) = 1. \quad (6.1)$$

t^* is the time to fracture of the rod, the dependence $f(\bar{c}_m)$ is an increasing function satisfying the equality $f(0) = 1$. By integrating (6.1), we can obtain the relationship between the time to failure in the absence and in the presence of an aggressive medium (t_0^* and t^* , respectively):

$$t_0^* = \left[(n + 1) A \sigma_0^n \right]^{-1} = \int_0^{t^*} f(\bar{c}_m(t)) dt. \quad (6.2)$$

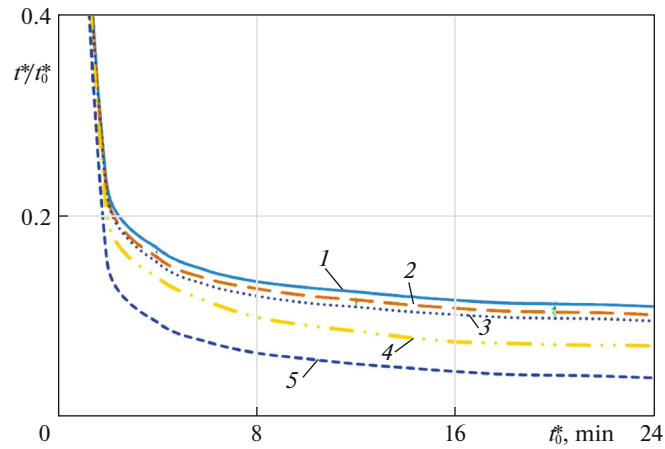


Fig. 5. Dependence of the ratio of time to failure in the presence and absence of an aggressive medium t^*/t_0^* on the time to failure in its absence t_0^* for rods with a hole with a different shape of the outer contour of the cross-section: 1—square cross-section, 2—rectangular cross-section $\alpha = 0.85$, 3—rectangular cross-section $\alpha = 0.7$, 4—a cross-section in the form of a ring, 5—a cross-section in the form of a thin rectangle with a hole.

In the case of a dependence $f(\bar{c}_m)$ with one material constant, a linear function can be considered [39]:

$$f(\bar{c}_m) = 1 + k\bar{c}_m; \quad k = 9.5. \tag{6.3}$$

Substituting the previously obtained dependences $\bar{c}_m(t)$ in (6.3), and then in (6.2), we obtain the times to fracture of rods of various shapes in an aggressive medium.

As an example, we will consider rods with holes at various shapes of cross-sections considered earlier in the article with a constant value of the area of these sections $F = 100 \text{ mm}^2$. These rods are made of α -Fe and are in a hydrogen environment at a temperature of 500°C ; in this case, the diffusion coefficient in the rod material is $D = 1.02 \text{ mm}^2/\text{min}$ [40].

Figure 5 shows the dependences of t^*/t_0^* on t_0^* (min) for the considered cross-sectional shapes. It follows from Fig. 5 that among the considered shapes of the cross-section of rods, the minimum time to failure corresponds to a rod with a two-connected cross-section in the form of a thin rectangular one with a hole.

Table 1 shows the values of times t^* and ratios t^*/t_0^* for all considered cross-sectional shapes at three values of t_0^* (6, 16, and 26 min). From Table 1 it follows that in rectangles, regardless of the value of t_0^* , the larger value of the length of the contour of the cross-section of the rectangle M corresponds to the smaller value of t^* . This means that an increase in the length of the contour of the cross-section of the rectangle M leads to a decrease in the time to failure t^* of the corresponding rod. So, among cross-sections in the form of rectangles with various combinations of sides, the time to fracture of the rods decreases with an increase in the value of the perimeter of the cross-section. This is true both for simply connected domains [4] and for two-connected domains.

CONCLUSIONS

Using an approximate solution of the diffusion equations, the characteristics of the diffusion process in the rods are determined for various shapes of their two-connected cross sections (circle, square, and rectangles with different aspect ratios). A variant of the kinetic theory of Yu.N. Rabotnov is used to determine the effect of an aggressive environment on the creep rupture strength of the stretched rods. Calculations show that the shortest time to failure is realized in rectangular rods with the minimum thickness b (at $\alpha = b/a = 0.0025$) among the considered ones. With the assumed equality of the areas of the considered cross-sections and the equality of tensile stresses, a rod with a rectangular cross-section with a minimum thickness is a rod with a cross-section having a maximum perimeter of the contour.

Table 1. Values of times t^* and ratios of times t^*/t_0^* for the considered two-connected shapes of the cross-section of the rod

No.	Cross-sectional shape with hole	Dimensions of the outer contour of the cross-section mm	M , mm	t^*/t_0^* , $t_0^* = 6$ min	t^*/t_0^* , $t_0^* = 16$ min	t^*/t_0^* , $t_0^* = 26$ min
1	Ring	$R = 15.642$	53.179	0.696	1.208	1.817
2	Square $a = 1$	$a = 10$	60.000	0.116	0.075	0.070
		$b = 10$		0.876	1.861	2.818
3	Rectangle. $\alpha = 0.90$	$a = 10.541$	60.084	0.146	0.116	0.108
		$b = 9.487$		0.846	1.802	2.734
4	$\alpha = 0.85$	$a = 10.846$	60.120	0.141	0.113	0.105
		$b = 9.220$		0.828	1.733	2.610
5	$\alpha = 0.80$	$a = 11.180$	60.330	0.138	0.311	0.100
		$b = 8.944$		0.783	1.635	2.502
6	$\alpha = 0.70$	$a = 11.952$	60.957	0.130	0.102	0.096
		$b = 8.367$		0.741	1.592	2.392
7	$\alpha = 0.60$	$a = 12.910$	61.968	0.124	0.100	0.092
		$b = 7.746$		0.719	1.324	2.110
8	$\alpha = 0.04$	$a = 50.000$	156	0.120	0.082	0.081
		$b = 2.000$		0.408	0.613	0.794
9	$\alpha = 0.0225$	$a = 66.667$	202.400	0.068	0.038	0.034
		$b = 1.500$		0.386	0.601	0.732
10	$\alpha = 0.01$	$a = 100$	303	0.064	0.038	0.028
		$b = 1$		0.354	0.583	0.699
11	$\alpha = 0.0025$	$a = 200$	600.500	0.059	0.036	0.027
		$b = 0.500$		0.312	0.537	0.632
				0.052	0.004	0.024

It is shown that among the sections in the form of hollow rectangles with various combinations of sides ($\alpha = 0.0025-0.9$), the time to failure of the rods decreases with a decrease in α and, as a result, with an increase in the value of the perimeter of the cross-section M .

The above conclusions on the dependences of the times to fracture on the perimeter for rods with cross-sections in the form of hollow rectangles are natural due to the similarity of the outer and inner contours of the sections.

The results of the times to fracture of similar hollow cross-sections of rods are not confirmed for the cross-sections in the form of a hollow square and a ring, considered in the article. The authors of the article explain this fact by the lack of similarity of the contours of these sections. With the assumed equality of the areas of all types of cross-sections considered in the article and the equality of tensile stresses, the time to failure of a rod with a cross-section in the form of a hollow square ($\alpha = 1$) exceeds the time to failure of a ring of the same area. For the considered times to failure under neutral conditions (6, 16, and 26 min), this excess is from 25 to 55 percent and increases with increasing time to failure. In this case, the length of the perimeter of the section in the form of a hollow square also exceeds the length of the perimeter of the ring. The authors explain this fact by the peculiarities of the diffusion process in the corners of the cross-section in the form of a hollow square.

FUNDING

This work partially supported by the Russian Science Foundation, project no. 19-19-00062.

REFERENCES

1. A. M. Lokoshchenko and L. V. Fomin, "Modeling the behavior of materials and structural elements exposed to aggressive media (review)," *Probl. Strength Plast.* **80** (2), 145–179 (2018).
2. A. M. Lokoshchenko, "Creep and long-term strength of metals in corrosive media (review)," *Mater. Sci.* **37**, 559–572 (2001).
3. A. M. Lokoshchenko and L. V. Fomin, "Influence of the cross-sectional shape of tensile bars on their creep rupture strength in a corrosive medium," *J. Appl. Mech. Tech. Phys.* **57**, 792–800 (2016).
4. N. S. Larin, A. M. Lokoshchenko, and L. V. Fomin, "Dependence of creep-rupture lifetime for rods under tension in an aggressive environment on the shape of a single-cell cross-section," *Mech. Solids* **54** (7), 1042–1050 (2019).
5. E. N. Vilchevskaya, A. B. Freidin, and N. F. Morozov, "Kinetics of the chemical reaction front in spherically symmetric problems of mechanochemistry," *Dokl. Phys.* **60**, 175–179 (2015).
6. A. B. Freidin, "On the chemical affinity tensor for chemical reactions in deformable materials," *Mech. Solids* **50**, 260–285 (2015).
7. E. N. Vilchevskaya, I. K. Korolev, and A. B. Freidin, "On phase transitions in a domain of material inhomogeneity. II. Interaction of a crack with an inclusion experiencing a phase transition," *Mech. Solids* **46**, 683–691 (2011).
8. I. I. Ovchinnikov, I. G. Ovchinnikov, and M. Yu. Bogina, "Modeling of deformation and fracture of materials under radiation exposure, taking into account the influence of the type of stress state. Report 1. On taking into account the effect of radiation exposure when constructing strain models under radiation conditions using the theory of structural parameters," *Internet Zh. Naukovedenie*, No. 2 (2013). <http://publ.naukovedenie.ru>.
9. Yu. N. Rabotnov, *Creep Problems in Structural Members* (North-Holland, Amsterdam, 1969).
10. I. G. Ovchinnikov, I. I. Ovchinnikov, M. Yu. Bogina, and A. V. Matora, "Models and methods used in the calculation and modeling of the behavior of structures exposed to radiation media," *Internet Zh. Naukovedenie*, No. 2 (2013). <http://publ.naukovedenie.ru>.
11. I. G. Ovchinnikov, M. Yu. Bogina, and A. V. Matora, "The influence of radiation media on the mechanical characteristics of materials and the behavior of structures (review)," *Internet Zh. Naukovedenie*, No. 4 (2012). <http://publ.naukovedenie.ru>.
12. B. Z. Margolin, A. G. Gulenko, I. P. Kursevich, and A. A. Buchatsky, "Prediction of the long-term strength of austenitic materials under neutron irradiation," *Vopr. Materialoved.*, No. 2 (42), 163–186 (2005).
13. B. Z. Margolin, A. A. Buchatskii, A. G. Gulenko, et al., "A method for predicting fracture resistance of material in cyclic loading under viscoelastoplastic deformation and neutron irradiation conditions," *Strength Mater.* **40**, 601–614 (2008).
14. F. M. Mitenkov, M. A. Bolshukhin, A. V. Kozin, Yu. G. Korotkikh, V. A. Panov, V. A. Pakhomov, and S. N. Pichkov, "Technology of operational monitoring of the resource of equipment and systems NPP," *Probl. Prochn. Plast.*, No. 74, 68–77 (2012).
15. A. S. Demidov, V. V. Kashelkin, A. D. Kashtanov, and V. A. Yakovlev, "Forecast of reactor steel 08Kh16N11MZ-PD mechanical properties under creep conditions with regard for irradiation and without irradiation," *Her. Bauman Moscow State Tech. Univ. Ser. Nat. Sci.*, No. 2 (2015).
16. G. M. Khazhinskii, *Behavior of Metal Nuclear Reactors* (Sputnik +, Moscow, 2018) [in Russian].
17. I. G. Ovchinnikov, V. V. Ratkin, and A. A. Zemlyanskii, *Modeling the Behavior of Reinforced Concrete Structural Elements under the Influence of Chloride-Containing Environments* (Saratov State Techn. Univ., Saratov, 2000) [in Russian].
18. I. G. Ovchinnikov and T. A. Khval'ko, *The Performance of Structures in Conditions of High-Temperature Hydrogen Corrosion* (Saratov State Techn. Univ., Saratov, 2003) [in Russian].
19. A. S. Kudryavtsev, V. G. Markov, and V. S. Lavrukhin, "Long-term strength of steel in a lead-based liquid metal coolant," *Vopr. Materialoved.*, No. 4 (48), 89–94 (2006).
20. A. S. Kudryavtsev, A. D. Kashtanov, V. G. Markov, and V. S. Lavrukhin, "Strength of chromium martensitic steel in a lead-based coolant," *Vopr. Materialoved.*, No. 1 (49), 78–82 (2007).
21. M. F. Chiang, H. H. Hsu, M. C. Young, and J. Y. Huang, "Mechanical degradation of cold-worked 304 stainless steel in salt spray environments," *J. Nucl. Mater.* **422**, 58–68 (2012).
22. O. K. Chopra and A. S. Rao, "A review of irradiation effects on LWR core internal materials – IASCC susceptibility and crack growth rates of austenitic stainless steels," *J. Nucl. Mater.* **409**, 235–256 (2011).
23. K. Fukuya, "Current understanding of radiation-induced creep of light water reactor structural materials," *J. Nucl. Mater.* **50**, 213–254 (2013).
24. F. A. Garner, B. J. Makenas, and S. A. Chastain, "Swelling and creep observed in AISI 304 fuel pin cladding from three MOX fuel assemblies irradiated in ERB-II," *J. Nucl. Mater.* **413**, 53–61 (2011).
25. J. Garnier, Y. Brechet, M. Delnondedieu, C. Pokor, P. Dubuissison, A. Renault, X. Averty, and J. P. Massoud, "Irradiating creep of SA 304L and CW 316 stainless steels: mechanical behavior and microstructural aspects. Part I. Experimental results," *J. Nucl. Mater.* **413**, 63–69 (2011).

26. B. A. Gurovich, E. A. Kuleshova, A. S. Frolov, D. A. Maltsev, K. E. Prikhodko, S. V. Fedotova, B. Z. Margolin, and A. A. Sorokin, "Investigation of high temperature annealing effectiveness for recovery of radiation-induced structural changes and properties of 18Cr-10Ni-Ti austenitic stainless steels," *J. Nucl. Mater.* **465**, 565–581 (2015).
27. E. Materna-Morris, A. Moslang, and H.-C. Schneider, "Tensile and low cycle fatigue properties of EURO-FER97-steel after 16.3 dpa neutron irradiation at 523, 623 and 723K," *J. Nucl. Mater.* **442**, 562–566 (2013).
28. J. Gupta, J. Hure, B. Tanguy, L. Laffont, M.-C. Lafont, and E. Andrieu, "Evaluation of stress corrosion cracking of irradiated 304L stainless steel in PWR environment using heavy ion irradiation," *J. Nucl. Mater.* **476**, 82–92 (2016).
29. M. Litao Chang, G. Burke, and F. Scenini, "Stress corrosion crack initiation in machined type 316L austenitic stainless steel in simulated pressurized water reactor primary water," *Corros. Sci.* **138**, 54–65 (2018).
30. M. Negyesi and Masaki Amaya, "The effect of nitride formation on the oxidation kinetics of Zry-4 fuel cladding under steam-air atmospheres at 1273-1573 K," *J. Nucl. Mater.* **524**, 263–277 (2019).
31. A. Renault-Laborne, J. Garnier, J. Malaplate, P. Gavoille, F. Sefta, and B. Tanguy, "Evolution of microstructure after irradiation creep in several austenitic steels irradiated up to 120 dpa at 320°C," *J. Nucl. Mater.* **475**, 209–226 (2016).
32. P. Lapouge, F. Onimus, M. Coulombier, J.-P. Raskin, T. Pardoën, and Y. Bréchet, "Creep behavior of submicron copper films under irradiation," *Acta Mater.* **131**, 77–87 (2017).
33. A. M. Lokoshchenko, *Creep and Creep Rupture of Metals in Aggressive Environments* (Moscow State Univ., Moscow, 2000) [in Russian].
34. A. M. Lokoshchenko, *Modeling of Creep and Creep Rupture of Metals* (Moscow State Industrial Univ., Moscow, 2007) [in Russian].
35. A. M. Lokoshchenko, *Creep and Long-Term Strength of Metals* (CISP. CRC Press, New York, 2018).
36. B. M. Budak, A. A. Samarskii, and A. N. Tikhonov, *Collection of Problems in Mathematical Physics* (Gos. Izd. Tekhiko-Tekhnicheskoi Literatury, Moscow, 1956) [in Russian].
37. M. M. Smirnov, *Problems on Mathematical Physics Equations* (Nauka, Moscow, 1968) [in Russian].
38. D. A. Kulagin, "A method for approximating two-dimensional diffusion equation solution," in *Proc. 3rd Int. Seminar "Modern Problems on Strength" (Staraya Russa, Sept. 20–24, 1999)* (Novgorod State Univ., Novgorod, 1999), Vol. 2, pp. 114–117 [in Russian].
39. L. V. Fomin, "Description of the creep rupture strength of tensile rods with rectangular and circular cross-sections at high-temperature air media," *Vestn. Samar. Gos. Tekh. Univ., Ser. Fiz.-Mat. Nauki*, No. 3 (32), 87–97 (2013).
40. P. V. Gel'd and R. A. Ryabov, *Hydrogen in Metals and Alloys* (Metallurgiya, Moscow, 1974) [in Russian].

Translated by V. Selikhanovich